Naval Research Laboratory

Washington, DC 20375-5320

NRL/MR/5651--20-10,094

The Noise Figure of Analog RF Photonic Receivers: Simple Links, WDM Links, and WDM Receive-Mode Beamformers

Frank Bucholtz

KeyW Corporation
Hanover, MD

Matthew J. Mondich

Joseph M. Singley

Jason D. McKinney

Keith J. Williams

Photonics Technology Branch
Optical Sciences Division

September 18, 2020

DISTRIBUTION STATEMENT A: Approved for public release; distribution is unlimited.

UNCLASSIFIED//DISTRIBUTION A

REPORT DOCUMENTATION PAGE

Form Approved
OMB No. 0704-0188

Public reporting burden for this collection of information is estimated to average 1 hour per response, including the time for reviewing instructions, searching existing data sources, gathering and maintaining the data needed, and completing and reviewing this collection of information. Send comments regarding this burden estimate or any other aspect of this collection of information, including suggestions for reducing this burden to Department of Defense, Washington Headquarters Services, Directorate for Information Operations and Reports (0704-0188), 1215 Jefferson Davis Highway, Suite 1204, Arlington, VA 22202-4302. Respondents should be aware that notwithstanding any other provision of law, no person shall be subject to any penalty for failing to comply with a collection of information if it does not display a currently valid OMB control number. **PLEASE DO NOT RETURN YOUR FORM TO THE ABOVE ADDRESS.**

1. REPORT DATE 09-20-2020

2. REPORT TYPE NRL Memorandum Report

3. DATES COVERED *(From - To)* 1 Nov 2019 – 15 Apr 2020

4. TITLE AND SUBTITLE
The Noise Figure of Analog RF Photonic Receivers: Simple Links, WDM Links, and WDM Receive-Mode Beamformers

5a. CONTRACT NUMBER

5b. GRANT NUMBER

5c. PROGRAM ELEMENT NUMBER 62271N

5d. PROJECT NUMBER

5e. TASK NUMBER EW-271-012

5f. WORK UNIT NUMBER 6B50

6. AUTHOR(S)
Frank Bucholtz*, Matthew J. Mondich, Joseph M. Singley, Jason D. McKinney, and Keith J. Williams

7. PERFORMING ORGANIZATION NAME(S) AND ADDRESS(ES)
Naval Research Laboratory
4555 Overlook Avenue, SW
Washington, DC 20375-5320

8. PERFORMING ORGANIZATION REPORT NUMBER
NRL/MR/5651--20-10,094

9. SPONSORING / MONITORING AGENCY NAME(S) AND ADDRESS(ES)
Office of Naval Research
One Liberty Center
875 North Randolph Street
Arlington, VA 22203-1995

10. SPONSOR / MONITOR'S ACRONYM(S) ONR

11. SPONSOR / MONITOR'S REPORT NUMBER(S)

12. DISTRIBUTION / AVAILABILITY STATEMENT
DISTRIBUTION STATEMENT A: Approved for public release; distribution is unlimited.

13. SUPPLEMENTARY NOTES
*KeyW Corporation, 7740 Milestone Pkwy, Suite 400, Hanover, MD 21076

14. ABSTRACT
In this report we compare the RF performance metrics of gain and noise figure for three analog RF photonic systems: a) a simple, single-laser, single-channel link; b) a single-channel link utilizing multiple laser sources; and c) a receive-mode RF photonic beamforming systems comprising multiple RF inputs and multiple laser sources. We discuss trade-offs at both the engineering level and the physics level.

15. SUBJECT TERMS
Photonics   Analog photonics   Microwave photonics
Noise figure   Beamformer   Fiber-optic links

16. SECURITY CLASSIFICATION OF:			17. LIMITATION OF ABSTRACT	18. NUMBER OF PAGES	19a. NAME OF RESPONSIBLE PERSON
a. REPORT	**b. ABSTRACT**	**c. THIS PAGE**			Joseph M. Singley
Unclassified Unlimited	Unclassified Unlimited	Unclassified Unlimited	Unclassified Unlimited	46	**19b. TELEPHONE NUMBER** *(include area code)* (202) 404-1012

Standard Form 298 (Rev. 8-98)
Prescribed by ANSI Std. Z39.18

(This page left blank)

Distribution Statement A. Approved for public release, distribution is unlimited.

Contents

Distribution Statement A. Approved for public release, distribution is unlimited.

(This page left blank)

Distribution Statement A. Approved for public release, distribution is unlimited.

1 EXECUTIVE SUMMARY

This report was motivated by recent work by M. Mondich, *et al* [1] of NRL who demonstrated a radio-frequency (RF) receive-mode beamforming system using a photonic architecture. An interesting challenge in the analysis of that system, comprising multiple RF inputs, is the calculation of noise figure. In an earlier NRL report we demonstrated a resolution of the issue of defining noise figure for a multiple-input RF system. In this report we apply those results to calculate the noise figure for the photonic beamforming system of Mondich. In addition, we compare the RF gain and noise figure of the beamformer system to two other well-known RF-photonic systems: a simple, single-laser, single-channel link; and a single-channel link employing an array of lasers as the optical source. We discuss the trade-offs among number of receive-array elements, number of beamformer modules, various noise contributions and system performance.

Distribution Statement A. Approved for public release, distribution is unlimited.

(This page left blank)

Distribution Statement A. Approved for public release, distribution is unlimited.

2 INTRODUCTION

Beamforming is a technique for determining the angle-of-arrival of a signal or, equivalently, for measuring the radio-frequency (RF) signal content in a solid angle along a particular direction in space. Systems employing a hybrid of RF and fiber-optical technologies offer unique advantages over purely-RF approaches. Among the benefits are a) true-time delay with extremely low RF attenuation over kilometers of delay lengths, b) use of the entire optical C-band to provide many terahertz of RF signal-processing bandwidth, and c) significantly reduced weight and volume compared to RF-only systems. As a practical matter, for long delays and for RF frequencies in the millimeter range and above, an RF photonic approach may provide the only viable solution. However, RF photonic systems often suffer from poor noise figure due to fundamental inefficiencies in converting between electrical and optical domains and back again. Hence, significant effort has been expended to improve the performance of RF photonic systems. The approaches include: 1) improving laser performance by increasing laser power and reducing laser noise, both while maintaining a small physical and electrical footprint; 2) improving photodetector performance by increasing power-handling capability and RF bandwidth while maintaining high conversion efficiency; and 3) improving system design by incorporating, for example, wavelength-division multiplexing (WDM) techniques to increase either optical power or to suppress optical noise.

Use of WDM techniques was shown to be effective in improving the noise factor in a single-channel RF photonic link [2]. Recently, Mondich [1] utilized a WDM array of laser sources in a receive-mode photonic beamforming system.

In 2006, Froberg [3] analyzed the impact of various combining techniques on the signal-to-noise ratio (SNR) of photonic beamformers, including beamformers that incorporate optical amplifiers. This report differs from the Froberg work in two important respects. First, we do not include optical amplifiers in our analysis since some applications of interest cannot tolerate the additional SWAP required by an array of optical amplifiers. Secondly, we believe the definition of input SNR used by Froberg is incorrect and can lead to a non-physical result for noise factor.

In this report we derive the noise factor for a receive-mode, RF photonic beamforming system of the type demonstrated by Mondich [1], a system that utilizes multiple, coherent RF inputs for spatial directivity and multiple, incoherent optical sources to both encode array element location onto optical wavelengths and to suppress RF instability due to optical interference effects.

Distribution Statement A. Approved for public release, distribution is unlimited.

Manuscript approved September 16, 2020.

Noise factor for a system is not measured directly but is calculated once RF gain and noise have been measured independently. For a single-input/single-output system: a) the RF gain can be measured directly by, for example, a vector network analyzer (VNA) to obtain the scattering coefficient S_{21} from which the power gain factor $G = |S_{21}|^2$; and b) the output noise power spectral density (PSD), N_{out}, can be measured directly using an electrical spectrum analyzer. Then the noise factor F is defined by

$$F = \frac{SNR_{in}}{SNR_{out}} = \frac{N_{out}}{Gk_BT_0} \tag{1}$$

where k_B is Boltzmann's constant and $T_0 = 290$ K is the standard temperature for noise figure.

In a system with multiple inputs, we expect to be able to measure the gain with respect to any one input, but how do we define gain for the entire system, that is, with signals and noise present at all M inputs? In an earlier report [4], we resolved the issue of the SNR definitions for a multiple-input/single-output RF system for a system of the type shown in Fig.1 and we showed that the proper definition of gain and of input SNR depended on whether the input RF signals were coherent or incoherent. Some of the results from that report will be utilized in Section 4.3 of this report.

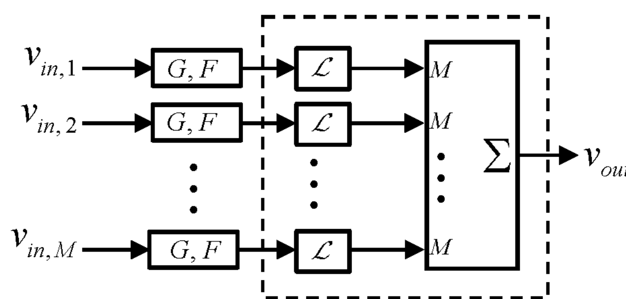

Figure 1: A purely-RF system with M parallel inputs having functionality similar to the RF photonic system in Fig. 2(c).(See Bucholtz [4]). G = gain factor, F = noise factor, $\mathcal{L}$ = loss factor, M = intrinsic power loss factor of the summing junction Σ.

In this report we always calculate RF noise in terms of electrical PSD (W/Hz) and we assume that, in the neighborhood of any RF frequency of interest, the noise PSD is relatively flat so conversion to noise power is accomplished simply by multiplication by the RF electrical bandwidth.

Thus, RF signal-to-noise ratios are always expressed in units Hz^{-1}. Although the logarithmic quantity *noise figure* $NF(dB)$ is the parameter most-typically quoted to describe device and system performance, here we shall calculate instead the more natural linear quantity *noise factor* F where $NF = 10\log_{10} F$. However, plots will all be made in terms of noise figure $NF(dB)$.

In order to facilitate comparisons among photonic systems we define a quantity I_{DC-S}, discussed below, which is the DC photocurrent due to a single laser source after modulation in a single modulator operating at the quadrature point. I_{DC-S} depends on the optical power from the laser, the responsivity of the photodetector and the optical loss in between the laser and the photodetector.

Finally we need to make some important comments about conventions and the definition of noise figure. RF components with a single input and single output come in two categories: active gain elements (amplifiers) and passive loss elements (attenuators). For amplifiers, the power gain factor G is defined as the ratio of output RF power to input RF power and where, by convention, $G \geq 1$. If the amplifier is turned off and $G \to 0$ then the gain is undefined. For attenuators, the gain factor is always less than one so, instead, we define a loss factor L as the ratio of input RF power to output RF power and where $L \geq 1$. To be sure, an RF system comprising multiple components can have an overall gain less than or equal to one, but each component in the system is categorized as either a gain or a loss element. In the RF domain, a single-channel RF photonic link, for all its internal complexity, comprises just a single-input / single-output RF device. But in stark contrast to purely-RF devices, the gain factor in an analog photonic link can be greater than one or less than one depending on a combination of system parameters, the most important of which is the laser optical output power. This feature of photonic links has important consequences for the calculation of output noise and, hence, of noise figure. In a purely-RF component the output thermal noise is $N_{out,therm} = \beta\,(N_{in} + k_B T_e)$ where $\beta = G$ or $\beta = 1/L$ depending on whether the component is an amplifier or attenuator, respectively, and where N_{in} is the noise at the device input and T_e is the noise-equivalent temperature of the device [4]. In calculating noise figure we must assume $N_{in} = k_B T_0$ and, if the device were ideal ($T_e = 0$) then the output noise is entirely amplified input noise. In a photonic link, the thermal contribution to the output noise $N_{out,therm} = (G+1)\,k_B T_0$ comprises both amplified input thermal noise and an additional $k_B T_0$. This additional term must be present because of the possibility that $G < 1$ in the photonic link. In the limit $G \to 0$, $N_{out,therm} \to k_B T_0$.

Distribution Statement A. Approved for public release, distribution is unlimited.

3 OVERVIEW

The three RF configurations to be analyzed in this report are shown in Fig. 2. Operating principles of the simple, single-channel link in Fig. 2(a) are well known. (See, for example, Urick [5], Cox [6] or Chang [7].) The WDM link in Fig. 2(b) is essentially the simple, single-channel link but with the single laser replaced by a WDM array of lasers to suppress the RIN (relative-intensity noise) contribution to RF noise at the output. Finally, the receive-beamformer architecture in Fig. 2(c) uses M lasers to encode the RF signals $v_{in,m}$ from each receiving element onto a single optical fiber for transmission to an array of K beamformer modules (BFMs) [1]. The goal of this report is to provide detailed derivations of the gain, noise and noise factor for the photonic beamformer system. Summaries of the same performance metrics for the other two systems are provided here for comparison.

Figure 1 shows an RF topology that we analyzed in an earlier report [4]. We see that the summing function inside the dotted box in Fig. 1 is here replaced with a significantly more complex electro-optical system inside the dotted box in Fig. 2(c). The added complexity and cost are happily borne because of the advantages offered by performing the delay and summation of signals entirely in the optical domain summarized above in the Introduction.

A complete list of symbols is provided in Appendix A.

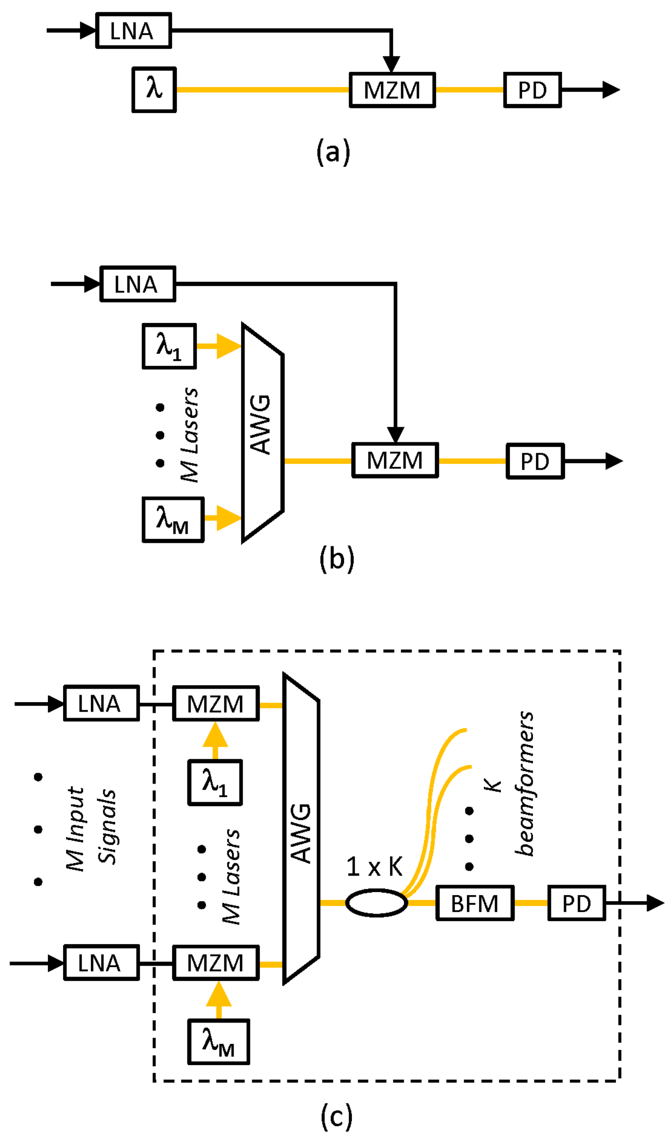

Figure 2: The three RF photonic configurations analyzed in this report. (a) Simple, single-channel link; (b) single-channel link with WDM source; (c) receive-mode beamformer employing multiple lasers. LNA = low noise (RF) amplifier, λ_m = wavelength of m-th laser, MZM = Mach-Zehnder modulator, PD = photodetector, AWG = arrayed-waveguide grating, $1\times K$ = fiber-optic splitter, and BFM = beamforming module. RF paths are shown in black and optical fiber paths are shown in yellow.

Distribution Statement A. Approved for public release, distribution is unlimited.

4 ANALYSIS OF RF PHOTONIC SYSTEMS

In this section we provide the results of RF noise factor analysis of each of the systems in Fig. 2. Results for the simple, single-channel link and for the single-channel WDM link will only be summarized since they have appeared previously in the literature. However, some details of the simple, single-channel system are provided in Appendix B. A detailed analysis for the beamformer architecture in Fig. 2(c) is presented in Section 4.3.

In the following we use upper case P to denote rms RF power and lower case p to denote rms optical power. We define a quantity κ that relates optical power to the magnitude squared of the scalar optical E-field E,

$$p = \frac{|E|^2}{2\kappa} \qquad or \qquad |E| = \sqrt{2\kappa p}. \tag{2}$$

4.1 Simple, single-channel link

Figure 3 shows a simple, single-RF-channel photonic link comprising a photonic section (inside the dotted box) driven by a conventional RF low-noise amplifier (LNA). We will first determine the noise factor of the photonic section alone with the input reference plane defined at the input to the Mach-Zehnder modulator (MZM). We then calculate the noise factor for the entire link using two approaches − a) the well-known formula for cascaded noise factors, and b) directly using the definition in Eq.(1). The following is a summary of terms used in this section.

$v_{lna} = v_{lna0} \sin(\Omega t - \psi)$ = LNA input RF voltage,
$v = v_0 \sin(\Omega t - \psi)$ = MZM input RF voltage,
i_{out} = output photocurrent,
Ω = RF (radian) frequency,
ψ = RF phase at MZM i/p,
θ = RF phase at PD i/p,
G_{lna} = RF power gain of LNA,
F_{lna} = noise factor of LNA = $\S_{21}|^2$,
λ = laser operating wavelength,
p = laser output optical rms power,
RIN = laser relative intensity noise,
V_π = MZM half-wave voltage,
$\alpha \geq 1$ is the optical power loss factor,

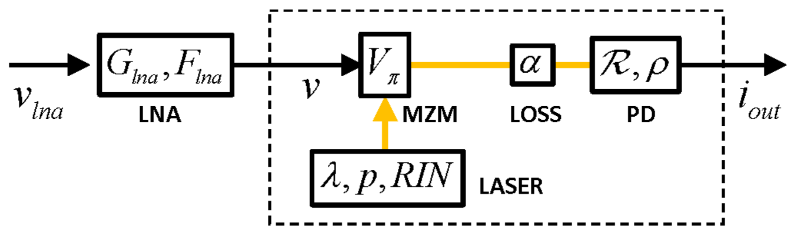

Figure 3: A simple, single-RF-channel photonic link comprising a low-noise amplifier (LNA), laser, Mach-Zehnder modulator (MZM), and photodetector (PD). Symbols are defined in the text.

PD = photodetector,
$\mathcal{R}$ = PD responsivity (A/W), and
ρ is a factor to account for the presence of an internal matching load inside the PD. Internal load: $\rho = 1/2$; no internal load: $\rho = 1$.

The loss factor α includes optical loss anywhere between the laser and the PD except for intrinsic loss in the MZM due to choice of operating point.

Some details of the analysis of the photonic portion of the link are provided in Appendix B. Here we summarize the results. The scalar optical field at the PD input is

$$E_{PD} = j\sqrt{\frac{2\kappa\, p}{\alpha}} \cos\frac{\phi}{2} \tag{3}$$

where ϕ is the phase shift impressed on the optical E-field by the MZM. $\phi = \phi_{bias} + \phi_{RF}$ and the RF phase shift is given by $\phi_{RF} = (\pi/V_\pi)\, v$.

Note: The MZM has two output ports and the expression in Eq.(3) corresponds to a particular choice of output port. If the other MZM output had been chosen, then $E_{PD} = j\sqrt{2\kappa p/\alpha} \sin(\phi/2)$.

The optical power at the PD input is

$$p_{PD} = \frac{|E_{PD}|^2}{2\kappa} = \frac{p}{\alpha}(1 + \cos\phi)\,. \tag{4}$$

If we assume the MZM is biased at quadrature ($\phi_{bias} = \pi/2$) and that the amplitude of the RF voltage v_0 is small enough that $\pi v_0/V_\pi << 1$, then

$$p_{PD} \rightarrow \frac{p}{\alpha}\left(1 + \frac{\pi}{V_\pi} v_0 \sin(\Omega t - \theta)\right). \tag{5}$$

The photocurrent at the PD output

$$\begin{aligned} i_{out} &= \frac{\mathcal{R}p}{\alpha}\left[1+\rho\left(\frac{\pi}{V_\pi}\right)v_0\sin\left(\Omega t-\theta\right)\right] \\ &= I_{DC-S}+i_{RF0}\sin\left(\Omega t-\theta\right), \end{aligned} \tag{6}$$

comprises a DC term and an RF term, where

$$I_{DC-S} = \left(\frac{\mathcal{R}p}{\alpha}\right) \tag{7}$$

and

$$i_{RF0} = I_{DC-S}\left(\frac{\pi\rho}{V_\pi}\right)v_0. \tag{8}$$

Note that the RF phase angle is now θ and not (the original) ψ to indicate that the RF phase will have changed as the signal propagates from the MZM input to the PD input.

Here we designate the DC photocurrent by "DC-S" to indicate it is the DC current for a simple, single-channel link, a designation that will facilitate performance comparisons among the three system types.

The RF power across output load impedance Z_{out} is

$$P_{out} = \frac{i_{RF0}^2 Z_{out}}{2} = \left(\frac{\pi^2\rho^2 Z_{in}Z_{out}}{V_\pi^2}\right)I_{DC-S}^2\left(\frac{v_0^2}{2Z_{in}}\right). \tag{9}$$

Since $P_{in} = v_0^2/2Z_{in}$ for MZM input load impedance Z_{in}, the RF gain of the photonic section is

$$G_{pho-S} = \frac{P_{out}}{P_{in}} = \left(\frac{\pi^2 Z_{in}Z_{out}\rho^2}{V_\pi^2}\right)\left(\frac{\mathcal{R}}{\alpha}p\right)^2 = \gamma I_{DC-S}^2 \tag{10}$$

where we define

$$\gamma \equiv \left(\frac{\pi^2 Z_{in}Z_{out}\rho^2}{V_\pi^2}\right). \tag{11}$$

Incidentally, note that the photonic portion of the link becomes transparent, $G_{pho-S} = 1$, when

$$I_{DC-S}\left(G_{pho-S}=1\right) = \frac{1}{\sqrt{\gamma}} = \frac{V_\pi}{\pi\rho\sqrt{Z_{in}Z_{out}}}. \tag{12}$$

So, for example, at $V_\pi = 4$ V, $Z_{in} = Z_{out} = 50$ ohms, and $\rho = 1/2$, we find $I_{DC-S}\left(G_{pho-S=1}\right) \simeq 50$ mA, a value well above the photocurrent that can be supplied by typical commercial diode lasers. Hence, bare photonic links typically operate at RF loss.

The output RF noise spectral density

$$N_{pho} = (1 + G_{pho-S})\, k_B T_0 + 2q\rho^2 Z_{out} I_{DC-S} + \rho^2 RIN \cdot Z_{out}\, I_{DC-S}^2 \quad (13)$$

comprises contributions from
a) output thermal noise $k_B T_0$,
b) amplified input thermal noise $G_{pho-S} k_B T_0$,
c) shot noise $2q\rho^2 Z_{out} I_{DC-S}$, and
d) relative intensity noise $\rho^2 Z_{out} RIN \cdot I_{DC-S}^2$.

Here, k_B is Boltzmann's constant, $T_0 = 290K$ is the standard temperature, q is the electron charge, and RIN is the RF power spectral density due to laser RIN normalized to $I_{DC-S}^2 Z_{out}$.

The noise factor is

$$F_{pho} = \frac{N_{pho}}{G_{pho-S} k_B T_0}. \quad (14)$$

Hence

$$F_{pho} = 1 + \frac{1}{\gamma} \left[\frac{1}{I_{DC-S}^2} + \left(\frac{2q\rho^2 Z_{out}}{k_B T_0} \right) \frac{1}{I_{DC-S}} + \left(\frac{\rho^2 Z_{out}}{k_B T_0} \right) RIN \right]. \quad (15)$$

We see that the contributions to F_{pho} due to output thermal noise and shot noise can be reduced by increasing the DC photocurrent but, for a single-laser link, the RIN contribution can be suppressed by increasing the γ factor, for example, by decreasing V_π or by reducing the RIN itself. But it should be remembered that reducing V_π degrades the spurious-free dynamic range [8].

Finally, for the entire end-to-end, simple, single-channel link, including the LNA, the gain is

$$G_S = G_{lna} G_{pho-S} \quad (16)$$

and, by the cascade formula for noise factors,

$$F_S = F_{lna} + \frac{F_{pho} - 1}{G_{lna}}. \quad (17)$$

Distribution Statement A. Approved for public release, distribution is unlimited.

The same result is obtained if, instead of using the cascade formula, we used Eq.(1) directly using the overall gain G_S in the denominator. But, in that case, we must account for the noise figure of the LNA, F_{lna}, and write the output noise as

$$N_S = (1 + G_{pho-S} G_{lna} F_{lna})\, k_B T_0 + 2q\rho^2 Z_{out} I_{DC-S} + \rho^2 RIN \cdot Z_{out} I_{DC-S}^2. \tag{18}$$

That is, in writing the output noise from only the photonic link, as we did in Eq.(15), we correctly assumed the MZM input noise was $k_B T_0$. However, once the LNA is connected, it is the noise at the LNA input that is $k_B T_0$ while the noise at the MZM input is now $G_{lna} F_{lna} k_B T_0$.

Hence, for the complete simple, single-channel link,

$$F_S = F_{lna} + \frac{1}{\gamma G_{lna}} \left[\frac{1}{I_{DC-S}^2} + \left(\frac{2q\rho^2 Z_{out}}{k_B T_0} \right) \frac{1}{I_{DC-S}} + \left(\frac{\rho^2 Z_{out}}{k_B T_0} \right) RIN \right]. \tag{19}$$

Figure 4 compares the noise figure NF as a function of DC photocurrent I_{DC-S} for the photonic link alone to the photonic link with an LNA at the MZM input. At large values of I_{DC-S} the NF is limited by the RIN of the laser and, since the RIN contribution to noise factor is independent of DC photocurrent, further increases in optical power provide no improvement. This flattening of the curve occurs for relatively low DC photocurrents. As the photocurrent approaches zero, the noise factor is dominated by shot and output thermal noises. Even for a relatively low RIN level at −150 dBc/Hz and large I_{DC-S} the noise factor for the bare photonic link is unacceptably large, and use of an LNA on the front end is typically necessary. But even then the NF is large by RF standards, especially for RIN levels > -150 dBc/Hz. One approach to reducing RIN is through the use of an array of independent lasers as the optical source.

4.2 Single-channel WDM link

Consider the link shown in Fig. 5 where, instead of a single laser source, an array of M lasers, each operating at a different wavelength, is used. (Because of its gross similarity to wavelength-division multiplexed digital

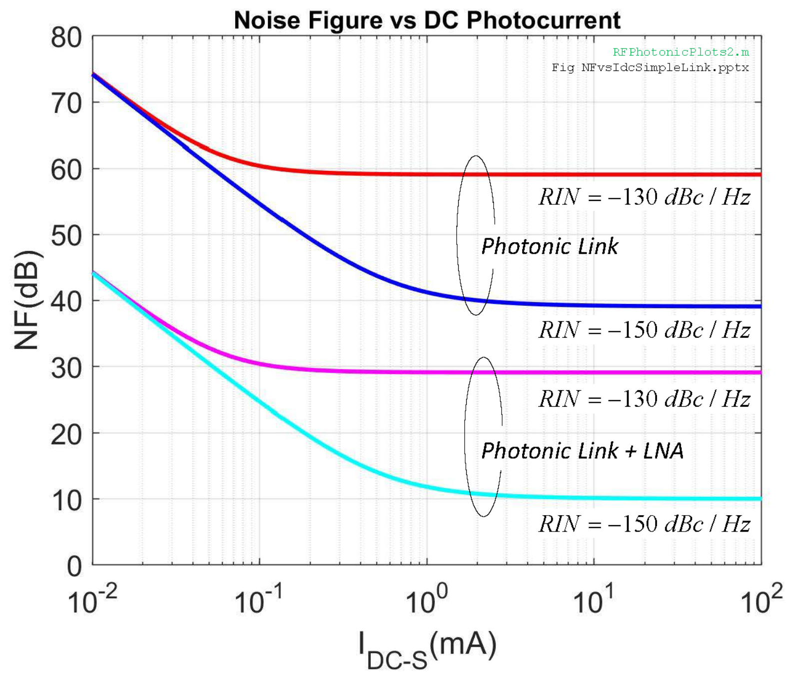

Figure 4: Noise figure versus DC photocurrent for the bare (no LNA) photonic link and for a link with an LNA at the MZM input (Refer to Fig. 3) at two RIN levels as indicated. For these plots: $V_\pi = 4$ V, $\rho = 1/2$, $T_0 = 290$ K, $Z_{in} = Z_{out} = 50$ ohms, $G_{lna} = 30$ dB and $NF_{lna} = 3.0$ dB.

communications systems, this architecture will be referred to as a WDM link.) We will see that multiple, independent lasers functioning as a single source act to suppress the RIN contribution to the output noise [2].

The gain of the photonic portion of the link, referenced to the MZM input, is

$$G_{pho-wdm} = \gamma \left(\sum_{m=1}^{M} I_{DC-S,m} \right)^2 , \tag{20}$$

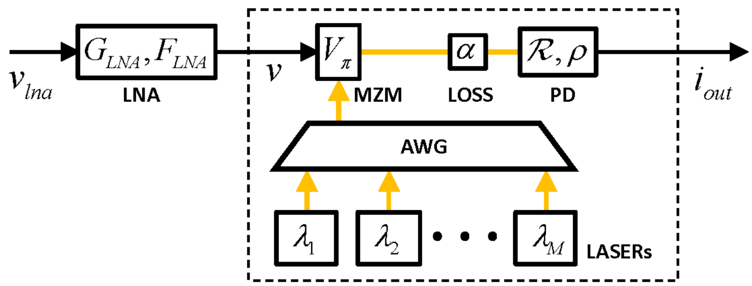

Figure 5: WDM link comprising a simple, single-channel link as in Fig. 3 but with the single laser replaced with an array of lasers. AWG = arrayed-waveguide grating.

the total output noise is

$$\begin{aligned} N_{pho-wdm} &= k_B T_0 \left(1 + G_{pho-wdm}\right) \\ &\quad + 2q\rho^2 Z_{out} \sum_{m=1}^{M} I_{DC-S,m} \\ &\quad + \rho^2 Z_{out} \sum_{m=1}^{M} RIN_m I_{DC-S,m}^2, \end{aligned} \tag{21}$$

and the general expression for the noise factor is

$$F_{pho-wdm} = \frac{N_{pho-wdm}}{G_{pho-wdm} k_B T_0}. \tag{22}$$

Assume now that each laser has the same output power as the single laser in the simple, single-channel system. Then the DC photocurrent is $M \cdot I_{DC-S}$ and the RF gain becomes

$$\begin{aligned} G_{pho-wdm} &\longrightarrow M^2 \gamma I_{DC-S}^2 \\ &\longrightarrow M^2 G_{pho-S}. \end{aligned} \tag{23}$$

Compared to the simple, single-channel link, the WDM link has M^2 larger gain.

After assuming the RIN of all lasers is the same, $RIN_m \rightarrow RIN$, the output RF noise PSD becomes

$$\begin{aligned} N_{pho-wdm} &\longrightarrow \left(1 + M^2 G_{pho-S}\right) k_B T_0 \\ &\quad + M\left(2q\rho^2 Z_{out}\right) I_{DC-S} \\ &\quad + M\left(\rho^2 \cdot RIN \cdot Z_{out}\right) I_{DC-S}^2. \end{aligned} \tag{24}$$

The benefit of this approach is seen clearly by comparing the gain in Eq. 23 with the RIN term in the output noise in Eq. 24. The gain has improved by M^2 but the shot and RIN contribution to the noise has increased by only M owing to the the fact that intensity noises from multiple, independent lasers add incoherently.

For the photonic portion of the single-channel WDM system, the noise factor becomes

$$F_{pho-wdm} \longrightarrow 1 + \frac{1}{\gamma}\left[\frac{1}{M^2}\frac{1}{I_{DC-S}^2} + \frac{1}{M}\left(\frac{2q\rho^2 Z_{out}}{k_B T_0}\right)\frac{1}{I_{DC-S}} + \frac{1}{M}\left(\frac{\rho^2 Z_{out}}{k_B T_0}\right) RIN\right]. \tag{25}$$

This result can be viewed in two ways. I) For fixed output power from each laser, increasing the number of lasers significantly improves the noise figure of the photonic portion of the system. The effect here is two-fold. Firstly, increasing the optical power increases $I_{DC-S}^2 \to M^2 I_{DC-S}^2$ which makes everything better. Secondly, in using an array of independent lasers as the source, the RIN contribution to the noise increases only linearly, not quadratically, with M [2]. II) Alternatively, we could consider keeping I_{DC-S} fixed and evaluate system performance for increasing M. That is, let $I_{DC-S} \to I_{DC-S}/M$. Then

$$F_{pho-wdm} \xrightarrow[I_{DC-S}\,fixed]{} 1 + \frac{1}{\gamma}\left[\frac{1}{I_{DC-S}^2} + \left(\frac{2q\rho^2 Z_{out}}{k_B T_0}\right)\frac{1}{I_{DC-S}} + \frac{1}{M}\left(\frac{\rho^2 Z_{out}}{k_B T_0}\right) RIN\right]. \tag{26}$$

In this case, for the same total DC photocurrent as in the simple, single-channel system, thermal and shot noise contributions to F remain unchanged but the RIN contribution has been suppressed by M.

If we now include the LNA on the front-end the overall RF gain for the end-to-end link is

$$G_{WDM} = G_{lna} G_{pho-wdm}, \tag{27}$$

Distribution Statement A. Approved for public release, distribution is unlimited.

and the noise factor

$$F_{WDM} = F_{lna} + \frac{F_{pho-wdm} - 1}{G_{lna}} \tag{28}$$

becomes

$$\begin{aligned} F_{WDM} = F_{lna} + \frac{1}{\gamma G_{lna}} \Bigg[& \frac{1}{I_{DC-S}^2} \\ & + \left(\frac{2q\rho^2 Z_{out}}{k_B T_0} \right) \frac{1}{I_{DC-S}} \\ & + \frac{1}{M} \left(\frac{\rho^2 Z_{out}}{k_B T_0} \right) RIN \Bigg] . \end{aligned} \tag{29}$$

The noise factor can be no smaller than the noise factor F_{lna} of the LNA, all the other contributions are suppressed by the LNA gain G_{lna}, and the RIN contribution can be further suppressed using multiple, incoherent lasers.

Some representative plots of gain and noise figure for the single-channel WDM systems are shown in Fig. 6. We see that reasonable noise figures can be obtained for $I_{DC-S} \geq 1$ mA and $M \geq 4$ provided $G_{lna} \sim 30$ dB and the noise factor of the LNA is reasonably low, say, $NF_{lna} \leq 3.0$ dB. Also, at low RIN levels, $I_{DC-S} \geq 1$ mA, and for the particular system parameters chosen here, increasing M beyond $M = 4$ provides little improvement in F.

Distribution Statement A. Approved for public release, distribution is unlimited.

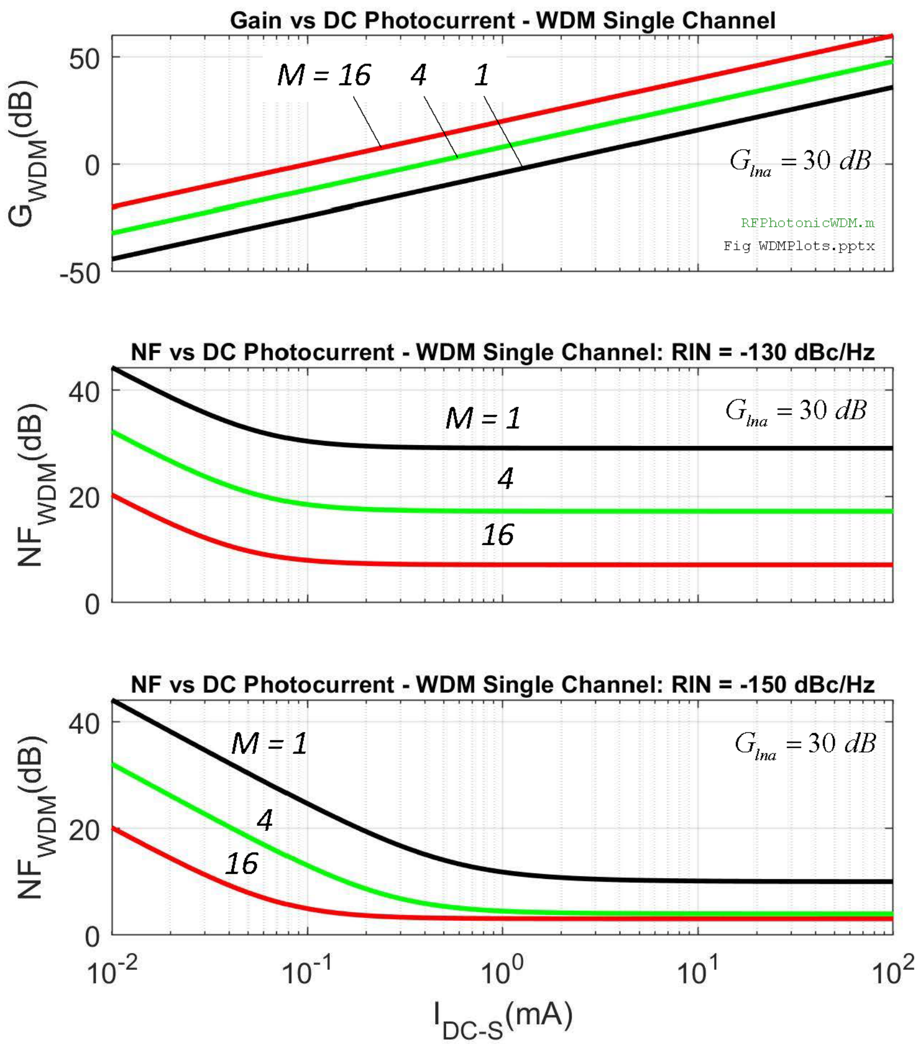

Figure 6: Top: Gain; Middle: NF for $RIN = -130$ dBc/Hz; Bottom: NF for $RIN = -150$ dBc/Hz. For these plots: $V_\pi = 4$ V, $\rho = 1/2$, $T_0 = 290$ K, $Z_{in} = Z_{out} = 50$ ohms, $G_{lna} = 30$ dB and $NF_{lna} = 3.0$ dB.

4.3 WDM Receive-Mode Beamformer

4.3.1 Receiver Beamformer with Multiple Inputs

In this section we analyze the multiple-laser receive-beamformer system shown in Fig. 2(c) which is reproduced in greater detail below in Fig. 7. The subsystem shown in the dotted box will be referred to as a beamformer module (BFM). Its purpose is to introduce carefully-chosen delays into each path so that, for some given angle-of-arrival of the RF wave incident on the receiver antenna array, the RF phases of the M optical signals reaching the PD all line up, that is, add constructively. The $1 \times K$ optical coupler divides the optical signal − containing RF information from all M array inputs − equally among the K BFMs.

It turns out that analysis of this system is reasonably straightforward, albeit a bit tedious. Wavelengths λ_m of the individual lasers are chosen such that difference frequencies occur well out of band of any RF signals of interest. At the same time, the RF signals arriving at the MZM inputs all come from a common RF wave as it washes across the receiving array. Each antenna array element provides a voltage that modulates the light from one laser, and that light follows a particular path through any of the beamformers and, without interacting with any of the other optical signals, eventually reaches the photodiode at the output of a BFM. Hence, this system is RF-coherent but optically-incoherent and this property simplifies the analysis considerably.

We only need to determine the noise factor F_{BF} for any one BFM output since that is really the only quantity of interest. The following is a list of symbols used in this section. It is the same list as for the simple, single-channel link but, here, with an index m, $1 \leq m \leq M$.

$v_{lna,m} = v_{lna0,m} \sin(\Omega t - \psi_m)$ = voltage at input to m^{th} LNA,
$v_m = v_{0m} \sin(\Omega t - \psi_m)$ = voltage input to MZM_m,
i_{out} = total output photocurrent,
$i_{out,m}$ = output photocurrent due to the $m - th$ path,
Ω = RF (radian) frequency,
ψ_m = RF phase in $m - th$ path at LNA input,
θ_m = RF phase in $m - th$ path at the position of the PD,
$G_{lna,m}$ = RF power gain of LNA_m,
$F_{lna,m}$ = noise factor of LNA_m,
λ_m = operating wavelength of m^{th} laser,
p_m = rms optical power at MZM_m,
RIN_m = laser m's relative intensity noise,

Distribution Statement A. Approved for public release, distribution is unlimited.

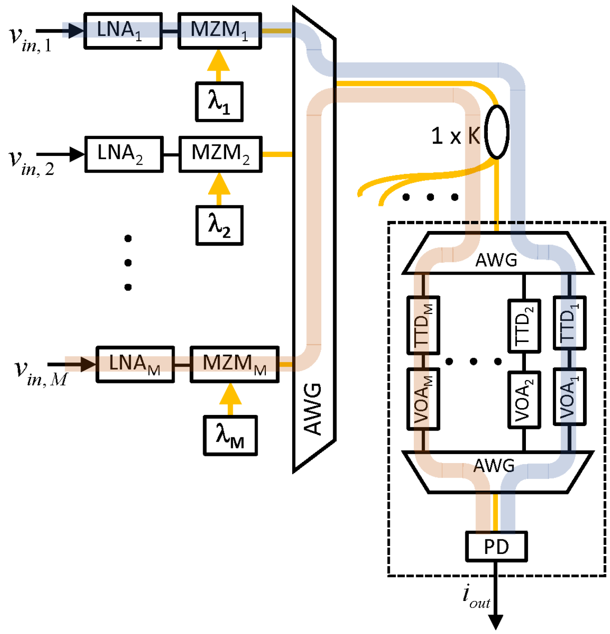

Figure 7: A receive-mode WDM beamformer system comprising a coherent RF system and an incoherent optical system. Light from a particular laser λ_m is modulated by the voltage $v_{in,m}$ incoming from the corresponding array element and propagates in the optical domain through the entire system without interacting with any other optical signals until reaching the photodetector PD. Two example paths are shown as heavy shaded lines. The subsystem in the dotted box is a beamformer module (BFM). A $1 \times K$ optical splitter distributes optical power equally among all K BFMs.

$V_{\pi,m}$ = half-wave voltage of MZM_m,
$\alpha_m \geq 1$ is the optical power loss factor in path m,
PD = photodetector,
$\mathcal{R}$ = PD responsivity, and
ρ is a factor to account for the presence of an internal matching load inside the PD. Internal load: $\rho = 1/2$; no internal load: $\rho = 1$.

The loss factor α_m accounts for all optical loss in the m^{th} path: insertion losses in the three AWGs, intentional shaping loss (variable optical attenuators, VOAs) in the BFM, and any other optical loss other than the intrinsic loss in the MZMs due to choice of operating point. α_m does not include the intrinsic loss of the $1 \times K$ coupler; this optical loss factor K will always be shown explicitly. The phase θ_m accounts for both phase differences due to angle-of-arrival of the incoming RF wave, as well as RF phase shifts introduced by the true-time delays (TTD$_m$) in the beamformer module.

We begin by calculating the RF gain for just the photonic portion of any one channel starting at an MZM input voltage $v_m = v_{0m} sin\,(\Omega t - \psi_m)$. When this signal reaches the photodetector it's RF phase becomes θ_m due to the intervening RF path length including, importantly, the RF true-time delays built into the BFM. The resultant photocurrent is given by Eq.(6)

$$\begin{aligned} i_{out,m} &= \frac{1}{K}\left(\frac{\mathcal{R}p_m}{\alpha_m}\right)\left[1 + \rho\left(\frac{\pi}{V_{\pi,m}}\right) v_{0m}\sin\left(\Omega t - \theta_m\right)\right] \\ &= I_{DC,m} + i_{RF,m} \end{aligned} \tag{30}$$

where

$$i_{RF,m} = i_{RF0,m}\sin\left(\Omega t - \theta_m\right) \tag{31}$$

and

$$i_{RF0,m} = \rho\left(\frac{\pi}{V_{\pi,m}}\right) v_{0m} I_{DC,m}, \tag{32}$$

and where the DC photocurrent here is decreased by the optical loss K of the $1 \times K$ optical splitter,

$$I_{DC,m} = \frac{1}{K}\left(\frac{\mathcal{R}p_m}{\alpha_m}\right) = \frac{1}{K} I_{DC-S,m}. \tag{33}$$

And where, similar to the definition in Eq.(7),

$$I_{DC-S,m} = \left(\frac{\mathcal{R}p_m}{\alpha_m}\right). \tag{34}$$

Finally, note that

$$v_{0m} = \sqrt{G_{lna,m}}\, v_{lna0,m}. \tag{35}$$

So the RF gain is

$$\begin{aligned} G_{pho,m} &= \frac{i_{RF0,m}^2 Z_{out}/2}{v_{0m}^2/2Z_{in}} \\ &= \frac{1}{K^2}\gamma_m I_{DC-S,m}^2 \end{aligned} \tag{36}$$

where (cf. Eq.(11))

$$\gamma_m = \left(\frac{\pi^2 Z_{in} Z_{out} \rho^2}{V_{\pi,m}^2}\right). \tag{37}$$

We next write an expression for the output noise PSD that includes the effect of the noise factor of the m^{th} LNA, $F_{lna,m}$. If we assume the noise input to the LNA is $k_B T_0$, then the noise out of the LNA is $G_{lna,m} F_{lna,m} k_B T_0$. This noise is then amplified by the photonic portion of the channel to produce a noise contribution $G_{pho,m} G_{lna,m} F_{lna,m} k_B T_0$ at the output. Hence, the output noise PSD due to just the m^{th} channel is

$$\begin{aligned} N_{bf,m} = G_{pho,m} G_{lna,m} F_{lna,m} k_B T_0 \\ + \frac{1}{K}\left(2q\rho^2 Z_{out}\right) I_{DC-S,m} \\ + \frac{1}{K^2}\left(\rho^2 Z_{out} \cdot RIN_m\right) I^2_{DC-S,m} \end{aligned} \tag{38}$$

or, writing the photonic gain explicitly in terms of $I_{DC-S,m}$ from Eq.(36), $G_{pho,m} = (\gamma_m / K^2) I^2_{DC-S}$,

$$\begin{aligned} N_{bf,m} = \frac{1}{K^2}\left(\gamma_m G_{lna,m} F_{lna,m} k_B T_0\right) I^2_{DC-S,m} \\ + \frac{1}{K}\left(2q\rho^2 Z_{out}\right) I_{DC-S,m} \\ + \frac{1}{K^2}\left(\rho^2 Z_{out} \cdot RIN_m\right) I^2_{DC-S,m}. \end{aligned} \tag{39}$$

We see that every term in the noise contribution from a particular path depends on the DC photocurrent.

Since the noise contributions are all mutually incoherent, the total output noise PSD is just the sum of all the individual PSDs, but with one additional term − we must add a single $k_B T_0$ to the output noise. That is, if the lasers are all turned off and the DC photocurrent goes to zero, $k_B T_0$ noise must still be present at the output. Hence, the total RF noise PSD at the output of any BFM is

$$\begin{aligned} N_{BF} = k_B T_0 + \frac{1}{K^2}\left(k_B T_0 \sum_{m=1}^{M} \gamma_m G_{lna,m} F_{lna,m} I^2_{DC-S,m}\right) \\ + \frac{1}{K}\left(2q\rho^2 Z_{out} \sum_{m=1}^{M} I_{DC-S,m}\right) \\ + \frac{1}{K^2}\left(\rho^2 Z_{out} \sum_{m=1}^{M} RIN_m \cdot I^2_{DC-S,m}\right). \end{aligned} \tag{40}$$

We now calculate the gain. Unlike the incoherent sum of noise contributions, the total output signal photocurrent is the coherent sum of the contributions from each path,

$$i_{out} = \sum_{m=1}^{M} i_{out,m} = \sum_{m=1}^{M} I_{DC,m} + \sum_{m=1}^{M} i_{RF,m} \tag{41}$$

and the rms output signal power at RF frequency Ω becomes

$$P_{out} = \left\langle \left| \sum_{m=1}^{M} i_{RF,m} \right|^2 \right\rangle Z_{out} \tag{42}$$

where brackets "$\langle\ \rangle$" indicate time average. (Note that there is no leading factor 1/2 here since that factor arises for a monochromatic wave only after taking the time average; it makes its appearance in this calculation anon.)

Performing the summation yields

$$\begin{aligned} &\left\langle \left| \sum_{m=1}^{M} i_{RF,m} \right|^2 \right\rangle \\ &= \left\langle \left(\sum_{m=1}^{M} i_{RF,m} \right) \left(\sum_{n=1}^{M} i_{RF,n} \right) \right\rangle \\ &= \left\langle \sum_{m,n=1}^{M} i_{RF,m} i_{RF,n} \right\rangle \\ &= \left\langle \sum_{m,n=1}^{M} i_{RF0,m} i_{RF0,n} \sin(\Omega t - \theta_m) \sin(\Omega t - \theta_n) \right\rangle. \end{aligned} \tag{43}$$

(Note: In the second line of the above equation we needed to use a second dummy index n when calculating the square of a sum of terms.) Using the trigonometric identity

$$\sin(\Omega t - \theta_m) \sin(\Omega t - \theta_n) = \frac{1}{2} \left[\cos(\theta_n - \theta_m) - \cos(2\Omega t + \theta_n + \theta_m) \right], \tag{44}$$

and we can ignore the second term, oscillating at 2Ω, since it time-averages to zero. Hence,

$$\left\langle \left| \sum_{m=1}^{M} i_{RF,m} \right|^2 \right\rangle = \frac{1}{2} \sum_{m,n=1}^{M} i_{RF0,m} i_{RF0,n} \cos(\theta_n - \theta_m). \tag{45}$$

Distribution Statement A. Approved for public release, distribution is unlimited.

This sum can be separated into two sums: a first sum where $m = n$ containing M terms, and a second sum, where $m \neq n$, containing $\left(M^2 - M\right)$ terms:

$$\begin{aligned} &\left\langle \left| \sum_{m=1}^{M} i_{RF,m} \right|^2 \right\rangle \\ &= \frac{1}{2} \left[\sum_{m=1}^{M} i_{RF0,m}^2 + \sum_{m \neq n=1}^{M} i_{RF0,m} i_{RF0,n} \cos\left(\Delta\theta_{nm}\right) \right] \\ &\equiv \frac{1}{2} \mathcal{B}(M) \end{aligned} \tag{46}$$

where $\Delta\theta_{nm} = (\theta_n - \theta_m)$ and where we define $\mathcal{B}(M)$ as the entire quantity in brackets on the right-hand side.

It is instructive at this point to consider the case where the amplitudes of all the RF photocurrents are equal $i_{RF0,m} = i_{RF0}\ \forall m$. Then

$$\mathcal{B}(M) = i_{RF0}^2 \left[M + \sum_{m \neq n=1}^{M} \cos\left(\Delta\theta_{nm}\right) \right]. \tag{47}$$

To "beamform" at some angle of incidence for the incoming RF wave means to adjust the TTDs in the BFM such that all the $\Delta\theta_{nm} = 0$. In this case, $\mathcal{B}(M)$ attains its maximum value

$$\mathcal{B}(M) = i_{RF0}^2 \left[M + M^2 - M \right] = M^2 i_{RF,0}^2 \tag{48}$$

and the output RF power is thus M^2 times the rms RF power from any one element.

$$P_{out} = M^2 \left(\frac{i_{RF0}^2 Z_{out}}{2} \right). \tag{49}$$

In general, however,

$$P_{out} = \mathcal{B}(M) Z_{out}/2 \tag{50}$$

where

$$\mathcal{B}(M) = \left[\sum_{m=1}^{M} i_{RF0,m}^2 + \sum_{m \neq n=1}^{M} i_{RF0,m} i_{RF0,n} \cos\left(\Delta\theta_{nm}\right) \right]. \tag{51}$$

Hence, the general expression for the beamformer system gain is

$$G_{BF} = \frac{\mathcal{B}(M) Z_{out}/2}{\sum_{m=1}^{M} v_{lna0,m}^2 / 2Z_{in}} \tag{52}$$

where $v_{lna0,m}$ is the voltage amplitude from the m^{th} array antenna element at the input to the LNA. Although completely accurate for computational purposes, this expression is not particularly helpful in understanding the general performance characteristics of the system.

Toward that end, let us again assume all the channels are equivalent and the phases are all properly aligned in the BFM. That is, for all m,

$v_{lna0,m} \to v_{lna0}$,
$G_{lna,m} \to G_{lna}$,
$F_{lna,m} \to F_{lna}$,
$p_m \to p$,
$RIN_m \to RIN$,
$V_{\pi,m} \to V_\pi$,
$\alpha_m \to \alpha$,
$I_{DC-S,m} \to I_{DC-S}$.

Then, by Eqs.(50) and (52), the gain becomes

$$G_{BF} \longrightarrow \frac{M^2 i_{RF0}^2 Z_{out}/2}{M v_{lna0}^2 / 2Z_{in}} = M \frac{i_{RF0}^2}{v_{lna0}^2} Z_{in} Z_{out}. \tag{53}$$

From Eq.(35) $v_0 = \sqrt{G_{lna}} v_{lna0}$ and from Eq.(32) $i_{RF0} = (1/K)(\pi\rho/V_\pi) v_0 I_{DC-S}$. Inserting these results into the gain equation yields, for the overall end-to-end system with equivalent channels,

$$\begin{aligned} G_{BF} &\longrightarrow M Z_{in} Z_{out} \frac{1}{K^2} \frac{\pi^2 \rho^2}{V_\pi^2} G_{lna} I_{DC-S}^2 \\ &\longrightarrow \frac{M}{K^2} \gamma G_{lna} I_{DC-S}^2. \end{aligned} \tag{54}$$

For the same system the output noise Eq.(40) becomes

$$\begin{aligned} N_{BF} \longrightarrow & k_B T_0 \left[1 + \frac{M}{K^2} \gamma G_{lna} F_{lna} I_{DC-S}^2 \right] \\ &+ \frac{M}{K} \left(2q\rho^2 Z_{out} \right) I_{DC-S} \\ &+ \frac{M}{K^2} \left(\rho^2 Z_{out} \cdot RIN \right) I_{DC-S}^2. \end{aligned} \tag{55}$$

Distribution Statement A. Approved for public release, distribution is unlimited.

Finally, the noise factor

$$F_{BF} = \frac{N_{BF}}{G_{BF} k_B T_0} \tag{56}$$

becomes

$$F_{BF} \longrightarrow F_{lna} + \frac{1}{\gamma G_{lna}} \left[\frac{K^2}{M} \frac{1}{I_{DC-S}^2} + K \left(\frac{2q\rho^2 Z_{out}}{k_B T_0} \right) \frac{1}{I_{DC-S}} + \left(\frac{\rho^2 Z_{out}}{k_B T_0} \right) RIN \right]. \tag{57}$$

This expression is very similar to the simple, single-channel result in Eq.(19) except for two terms that are modified by the factors M and K: the output thermal noise term is multiplied by K^2/M and the shot noise term is multiplied by K. Otherwise, all the other terms are just the single-channel factors.

We see immediately that, although the beamformer system utilizes M laser sources, it does not enjoy the suppression of RIN seen in the WDM link Eq.(29). In that WDM system, all M lasers were brought to bear on a single MZM and, hence, on a single RF channel. In the beamformer system, each laser drives its own MZM so the beneficial effect of mutual incoherence of laser RINs is lost. However, the great benefit of independent lasers here is that the system is guaranteed to be optically incoherent and, thus, free of RF instabilities due to optical interference effects.

As expected, in the limit $K, M \to 1$, F_{BF} reduces to F_S, the simple, single-channel noise factor in Eq.(19). In the limit of large I_{DC-S}, F_{BF} is limited by laser RIN and, ultimately, by the noise factor of the low-noise amplifier.

$$F_{BF} \xrightarrow[I_{DC-S}\to\infty]{} F_{lna} + \frac{1}{\gamma G_{lna}} \left(\frac{\rho^2 Z_{out}}{k_B T_0} \right) RIN. \tag{58}$$

In the low photocurrent regime, $I_{DC-S} \to 0$, two contributions dominate, namely, output thermal noise and shot noise

$$F_{BF} \xrightarrow[I_{DC-S}\to 0]{} \frac{1}{\gamma G_{lna}} \left[\frac{K^2}{M} \frac{1}{I_{DC-S}^2} + K \left(\frac{2\rho^2 Z_{out}}{k_B T_0} \right) \frac{1}{I_{DC-S}} \right]. \tag{59}$$

In the intermediate regime, the degree of degradation of F_{BF} due to $M, K \neq 1$ depends on the values of all the other parameters, including I_{DC-S}. These effects are seen in Fig. 8.

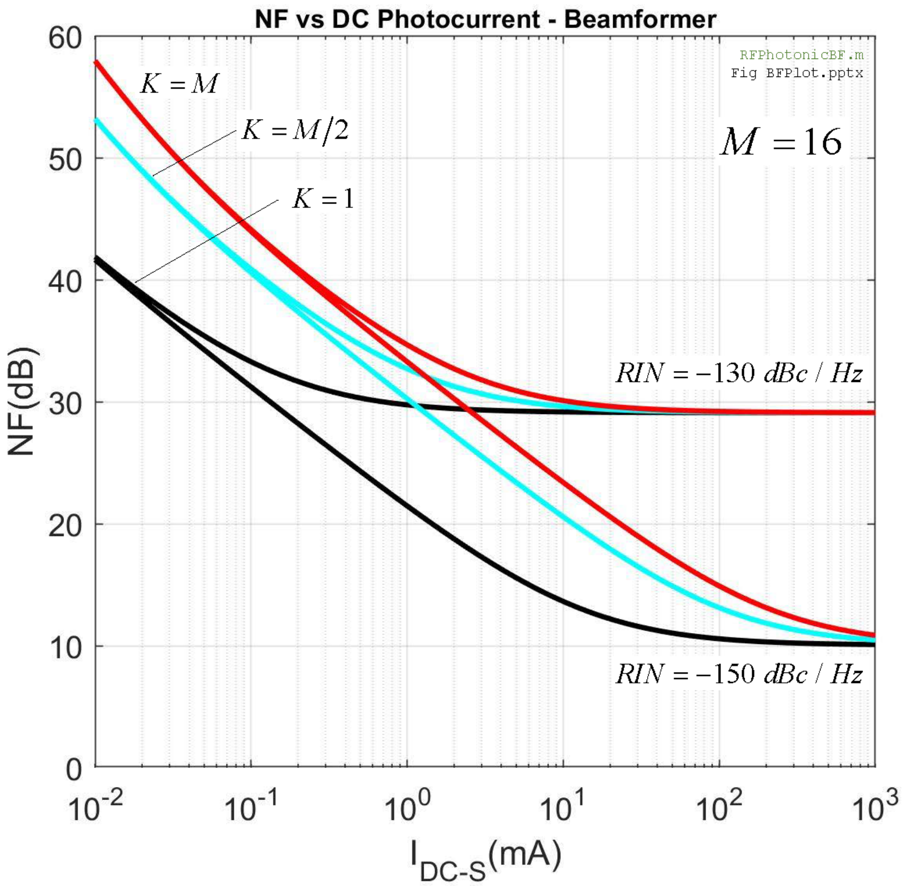

Figure 8: Noise figure as a function of I_{DC-S} for a beamformer with $M = 16$ receive-array elements and K BFMs for RIN = -130 dBc/Hz and RIN = -150 dBc/Hz. For these plots: $V_\pi = 4$ V, $\rho = 1/2$, $T_0 = 290$ K, $Z_{in} = Z_{out} =$ 50 ohms, $G_{lna} = 30$ dB and $NF_{lna} = 3.0$ dB.

4.3.2 Receiver Beamformer with Inputs Derived from a Single Source

A natural way to measure the gain of the beamformer system is to use a vector network analyzer and an RF splitter, such as a Wilkinson divider, to provide voltages at each of the M inputs as shown in Fig. 9.

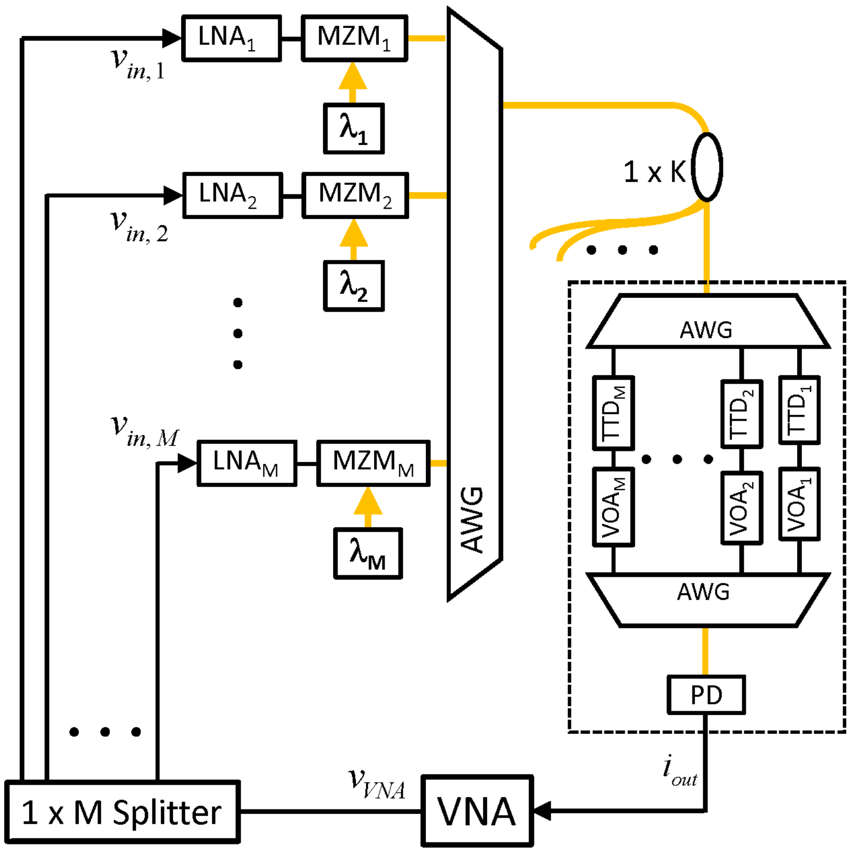

Figure 9: Test set-up for a receive-beamformer system using a vector network analyzer (VNA) and a Wilkinson-type $1 \times M$ RF splitter.

It is of interest to understand how the performance of this system scales with the number M of receive-array elements. Such a measurement could be performed in two ways as shown in Fig. 10. In the first approach, the amplitude of v_{vna} is fixed and we insert splitters with successively larger tap numbers $M = 2, 4, 8, \cdots$, for example, and measure the gain as a function of M. In the second approach, we keep both the amplitude of v_{vna} and the

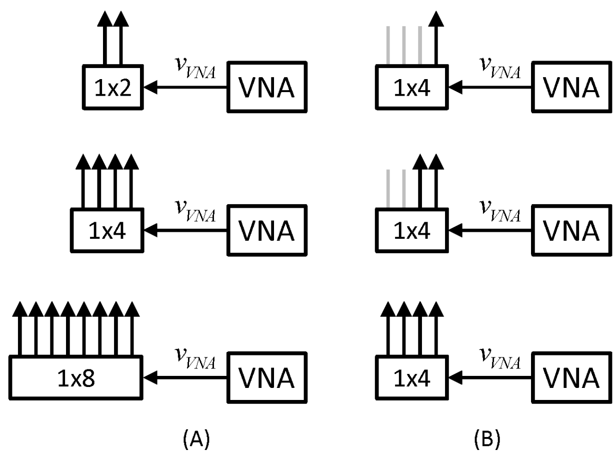

Figure 10: Two approaches for determining how the gain of the beamformer scales with number M of receive-array elements. (A) Vary the size of the splitter, and (B) Fix the size of the splitter but vary the number of output ports connected to the beamformer.

number of splitter taps M fixed, but we only connect $M' \leq M$ of the splitter outputs at a time, properly terminating the unconnected outputs, and measure gain as a function of M'. These two measurements yield different answers!

We will calculate first the gain for approach (A) even though this method is entirely impractical as it would require rebuilding the entire system with each change in M. This calculation answers the question "If the beamformer is built with M array elements, what is the gain?" The second approach is very accessible experimentally but it answers a different question, namely, "For a fixed system architecture, how does the gain change as the number of array elements that receive radiation is changed?" It is perhaps unsurprising then that different questions produce different answers.

To determine the gain for approach (A) note that the Wilkinson device divides power equally among all M outputs and, hence, divides input voltage by $\sqrt{M}$ so $v_{lna0,m} = v_{vna0}/\sqrt{M}$.

Assuming that all channels are equivalent, we can insert this result directly into Eqs.(32) $-$ (35) to obtain

$$i_{RF0,m} \longrightarrow \left(\frac{\pi\rho\sqrt{G_{lna}}}{V_\pi}\right) \frac{I_{DC-S}}{K} \frac{v_{vna0}}{\sqrt{M}}. \tag{60}$$

As before, we assume the beamformer module is arranged to maximize the sum $\mathcal{Q}(M) = M^2 - M$ in which case

$$\mathcal{B}(M) = M^2 i_{RF0}^2. \tag{61}$$

The output power is

$$P_{out} = \frac{1}{2} M^2 i_{RF0}^2 Z_{out} = \frac{M}{K^2} G_{pho-S} G_{lna} P_{in} \tag{62}$$

for input power $P_{in} = v_{vna0}^2 Z_{in}/2$.

So, finally, the gain is

$$G_{BF} = \frac{M}{K^2} G_{pho-S} G_{lna} = \frac{M}{K^2} \gamma G_{lna} I_{DC-S}^2 \tag{63}$$

which is exactly the gain we obtained earlier in Eq.(54). The reason is clear. In the multiple-input case, as we argued in the earlier report [4], the correct input power to use is the sum of the input RF powers on all the array elements. But the sum of the input powers in this case is just the output power from the VNA. Perhaps more remarkable is the fact that the gain scales linearly with M. In fact, why should the gain depend at all on M? After all, the total input power from the VNA is fixed and the power divider only distributes that constant power over different numbers of elements. The reason stems from the coherent addition of currents that occurs in the photodiode, that is, from the nature of interferometric RF mixing.

In Approach (B) in which, say, only M' of the M inputs are present, we note the following. The input power from the VNA does not change with M' but $\mathcal{B}(M)$ is now $\mathcal{B}(M') = M'^2 i_{RF0}^2$ and, as a result, the gain is

$$G'_{BF} = \frac{M'^2}{K^2 M} G_{pho-S} G_{lna}. \tag{64}$$

Since $M' \leq M$, $G'_{BF} \leq G_{BF}$, as must be the case. But we see that G'_{BF} *increases* with M'^2 that is, with the square of the number of inputs that are connected. This dependence of gain on M'^2 was observed by Mondich [1].

Finally, what about noise in Approach (B)? For this system, the output noise is entirely agnostic to the manner in which input signals are applied. Hence, regardless of whether approach (A) or (B) is used to measure gain, the output noise PSD for equivalent channels is given by Eq.(55). However, we must assume in approach (B) that, if only M' input ports are connected then only M' lasers are turned on in which case there are only M' contributions to the output thermal noise, the shot noise, and the RIN. Mondich [1] also observed this change in noise with M'.

5 Summary and Discussion

Figure 11 is a comparison of the expressions for gain, noise PSD, and noise factor for the three architectures analyzed in this report under the assumption that all channels are equivalent. Here $I_{DC-S} = \mathcal{R}p/\alpha$ and $\gamma = \pi^2\rho^2 Z_{in}Z_{out}/V_\pi^2$. Recall that all these performance metrics are defined with respect to the output of a single beamformer module, that is, just one of the K BFMs. Some notable features for the performance of the beamformer system are the following.

1) By using multiple, independent laser sources, the photonic receive beamformer system is RF coherent but optically incoherent thus eliminating RF instability due to optical interference.

2) To calculate gain and noise factor for a system with coherent RF inputs, the input RF power must be properly defined as the *total* combined RF power from all receive elements [4].

3) Both the total input RF power from the M receive-array elements and the total optical power from the M lasers are divided up among the K BFMs and this splitting occurs in the optical domain. Hence, K has a significant deleterious effect on performance.

4) In the single-channel WDM system discussed in this report for comparison purposes, a significant reduction in the RIN contribution to noise factor was achieved due to the incoherent summation of RINs from M independent lasers. In the beamformer system, however, although M independent lasers were utilized, each laser provided the carrier for only one of M RF channels. As a result, the noise factor of the beamformer does not improve with M.

5) In the case where all the channels have equivalent RF and optical characteristics, the form of the expressions for gain, noise and noise factor are very similar to the case of just one equivalent channel, but with each term in an expression worsened by a function of M and K. For example, the gain of a single, equivalent channel is $G_S = \gamma G_{lna} I_{DC-S}^2$ while the gain at a BFM output, assuming the lasers all emit the same optical power as in the single-channel system, is only $G_{BF} = (M/K^2)\gamma G_{lna} I_{DC-S}^2$.

6) In a subtle but important distinction, the method in which gain is measured as a function of the number of RF channels strongly affects the result as discussed in Sect. 4.3.2. Hence, care must be taken in the comparison of theory and measurement.

Distribution Statement A. Approved for public release, distribution is unlimited.

	RF Gain	**Noise PSD**	**Noise Factor**
Simple, Single-Channel Link	$G_S = G_{lna} G_{pho-S} = \gamma G_{lna} I_{DC-S}^2$	$N_S = k_B T_0 \left(1 + \gamma G_{lna} F_{lna} I_{DC-S}^2\right) + 2q\rho^2 Z_{out} I_{DC-S} + \rho^2 Z_{out} RIN \cdot I_{DC-S}^2$	$F_S = F_{lna} + \frac{1}{\gamma G_{lna}}\left[\frac{1}{I_{DC-S}^2} + \left(\frac{2q\rho^2 Z_{out}}{k_B T_0}\right)\frac{1}{I_{DC-S}} + \left(\frac{\rho^2 Z_{out}}{k_B T_0}\right) RIN\right]$
Single Channel -WDM (M lasers)	$G_{WDM} = M^2 G_{lna} G_{pho-S} = M^2 \gamma G_{lna} I_{DC-S}^2$	$N_{WDM} = k_B T_0 \left(1 + M^2 \gamma G_{lna} F_{lna} I_{DC-S}^2\right) + M\left(2q\rho^2 Z_{out}\right) I_{DC-S} + M\left(\rho^2 Z_{out}\right) RIN \cdot I_{DC-S}^2$	$F_{WDM} = F_{lna} + \frac{1}{\gamma G_{lna}}\left[\frac{1}{M^2}\frac{1}{I_{DC-S}^2} + \frac{1}{M}\left(\frac{2q\rho^2 Z_{out}}{k_B T_0}\right)\frac{1}{I_{DC-S}} + \frac{1}{M}\left(\frac{\rho^2 Z_{out}}{k_B T_0}\right) \cdot RIN\right]$
Beamformer (M Rx elements) (M lasers) (K beamformers)	$G_{BF} = \frac{M}{K^2} \cdot G_{lna} G_{pho-S} = \frac{M}{K^2} \cdot \gamma G_{lna} I_{DC-S}^2$	$N_{BF} = k_B T_0 \left(1 + \frac{M}{K^2} \gamma G_{lna} F_{lna} I_{DC-S}^2\right) + \frac{M}{K}\left(2q\rho^2 Z_{out}\right) I_{DC-S} + \frac{M}{K^2}\left(\rho^2 Z_{out}\right) \cdot RIN \cdot I_{DC-S}^2$	$F_{BF} = F_{lna} + \frac{1}{\gamma G_{lna}}\left[\frac{K^2}{M}\frac{1}{I_{DC-S}^2} + K\left(\frac{2q\rho^2 Z_{out}}{k_B T_0}\right)\frac{1}{I_{DC-S}} + \left(\frac{\rho^2 Z_{out}}{k_B T_0}\right) \cdot RIN\right]$

Figure 11: Summary of expressions. $M =$ of array elements, $K =$ of beamformer modules.

Figures 12 and 13 compare the gain and noise figure as a function of I_{DC-S} for the three system designs assuming reasonable, practical values for operational parameters as specified in the caption and, in the beamformer case, assuming all channels are equivalent. From Fig. 12 we see that the WDM system exhibits the largest gain at all levels of DC photocurrent because, as discussed in the previous section, the optical power from all M lasers is modulated by the single RF signal. Interestingly, the beamformer gain for $K = 1$ is significantly larger than the gain of the simple, single-channel system owing to effects of coherent addition of the RF signals at the PD. But for $K > \sqrt{M}$ the beamformer gain is always smaller than the single-channel gain.

Figure 13 compares the behavior of the noise figures. We see that, in the limit of large I_{DC-S}, the $K = 1$ beamformer has the same NF as the simple, single-channel link. Otherwise, the noise factor worsens linearly with K. At low-enough RIN, the NF is limited by K times the shot-noise limit which, in the case of an $M = 16$ WDM link, can approach the ultimate system limit, namely, NF_{lna}.

Finally, Figure 14 summarizes the general expressions for the beamformer RF metrics.

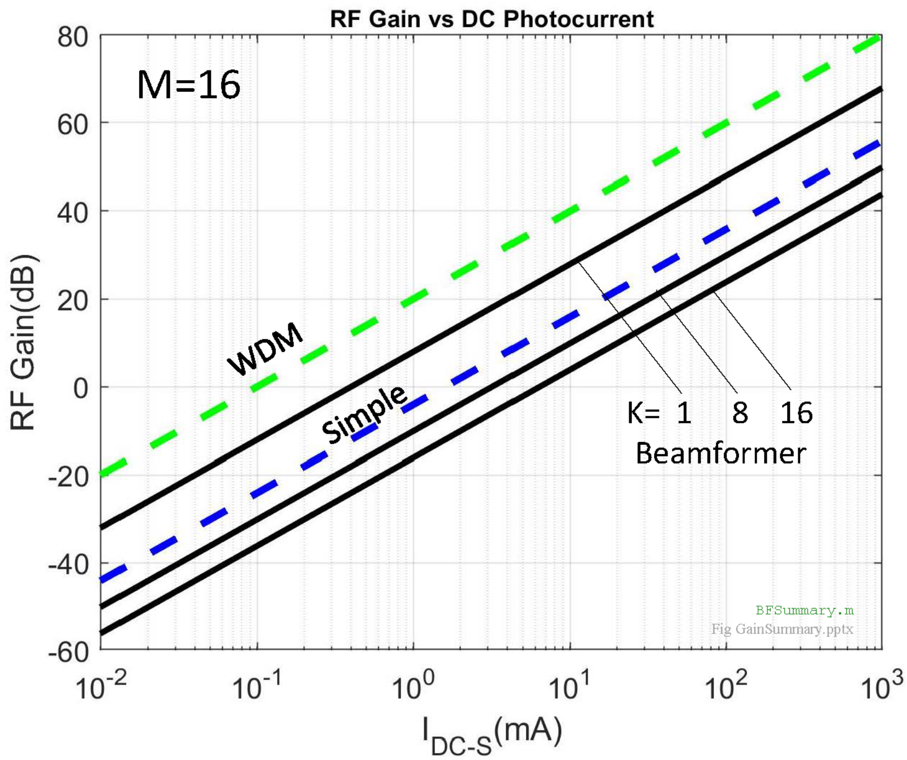

Figure 12: Gain as a function of I_{DC-S} for a beamformer with $M = 16$ receive-array elements and K BFMs. For these plots: $V_\pi = 4$ V, $\rho = 1/2$, $T_0 = 290$ K, $Z_{in} = Z_{out} = 50$ ohms and $G_{lna} = 30$ dB.

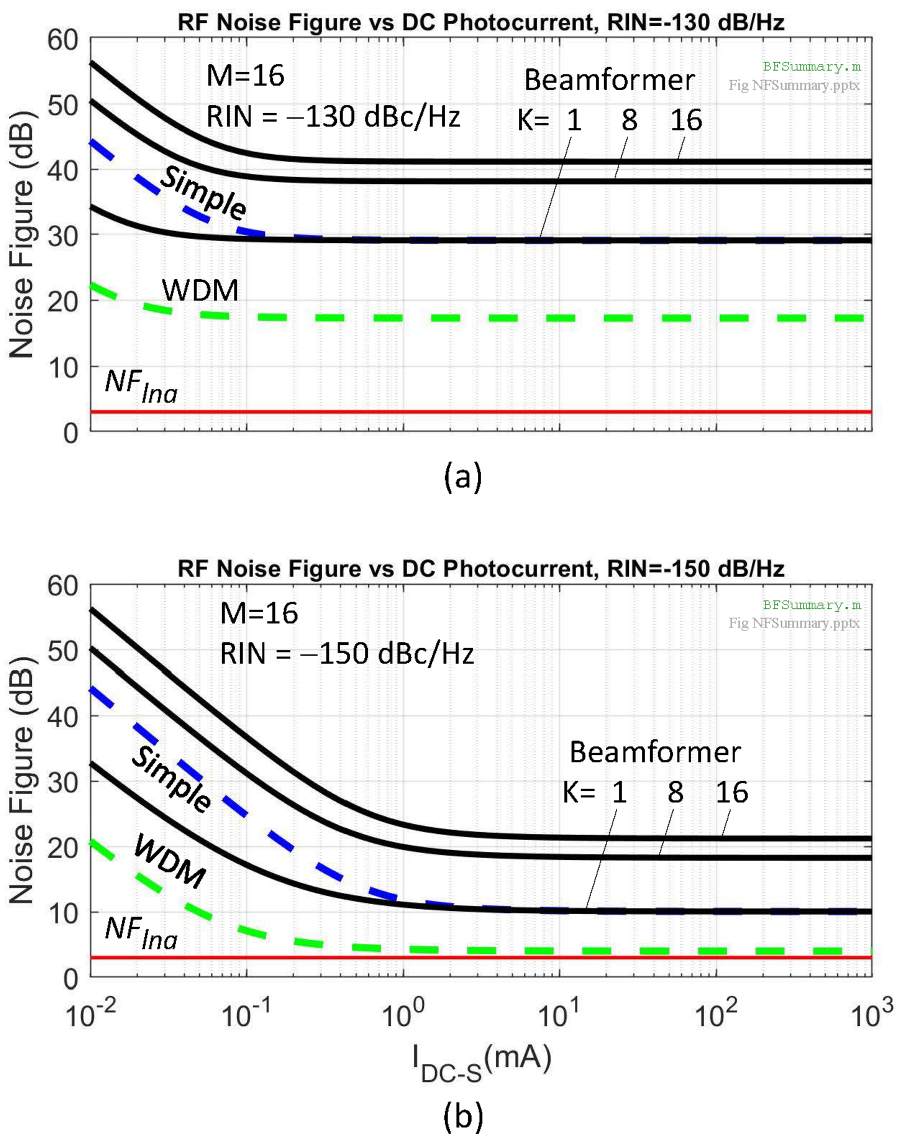

Figure 13: Noise figure as a function of I_{DC-S} for (a) RIN = -130 dBc/Hz and (b) RIN = -150 dBc/Hz. For these plots: $V_\pi = 4$ V, $\rho = 1/2$, $T_0 =$ 290 K, $Z_{in} = Z_{out} = 50$ ohms, $G_{lna} = 30$ dB and $NF_{lna} = 3.0$ dB. For the beamformer plots, $M = 16$ receive-array elements and $K = 1$, $M/2$, and M BFMs.

Gain $$G_{BF} = \frac{\mathcal{B}(M) Z_{out} / 2}{\sum_{m=1}^{M} v_{lna0,m}^2 / 2Z_{in}}$$

where $$\mathcal{B}(M) = \sum_{m=1}^{M} i_{RF0,m}^2 + \sum_{m \neq n = 1}^{M} i_{RF0,m} i_{RF0,n} \cos \Delta\theta_{mn}$$

and $$\begin{cases} \Delta\theta_{mn} = \theta_m - \theta_n \\ i_{RF0,m} = \dfrac{\sqrt{G_{lna,m}}}{K} \left(\dfrac{\pi\rho}{V_{\pi,m}} \right) \left(\dfrac{Rp_m}{\alpha_m} \right) v_{lna0,m} \end{cases}$$

Noise PSD $$N_{BF} = k_B T_0 \left[1 + \frac{1}{K^2} \sum_{m=1}^{M} \gamma_m G_{lna,m} F_{lna,m} I_{DC-S,m}^2 \right] + \frac{1}{K} \left(2q\rho^2 Z_{out} \right) \sum_{m=1}^{M} I_{DC-S,m} + \frac{1}{K^2} \left(\rho^2 Z_{out} \right) \sum_{m=1}^{M} RIN_m \cdot I_{DC-S,m}^2$$

Noise Factor $$F_{BF} = \frac{1}{G_{BF}} \left[\left(1 + \frac{1}{K^2} \sum_{m=1}^{M} \gamma_m G_{lna,m} F_{lna,m} I_{DC-S,m}^2 \right) + \frac{1}{K} \left(\frac{2q\rho^2 Z_{out}}{k_B T_0} \right) \sum_{m=1}^{M} I_{DC-S,m} + \frac{1}{K^2} \left(\frac{\rho^2 Z_{out}}{k_B T_0} \right) \sum_{m=1}^{M} RIN_m \cdot I_{DC-S,m}^2 \right]$$

Figure 14: General expressions for the photonic beamformer RF metrics. M = of array elements, K = of beamformer modules.

Distribution Statement A. Approved for public release, distribution is unlimited.

A APPENDIX A: LIST OF SYMBOLS

$B = RF$ bandwidth.

$BF =$ beamformer.

$BFM =$ beamformer module.

$DC =$ direct current

$E =$ scalar electric field.

$F =$ noise factor.

$F_{lna} =$ noise factor of LNA.

$F_{lna,n} =$ noise factor of $m-th$ LNA.

$F_{pho-S} =$ noise factor of simple, single-channel link wrt MZM i/p.

$F_{pho-wdm} =$ noise factor of single-channel WDM link wrt MZM i/p.

$F_{pho-bf} =$ noise factor of photonic-only portion of beamformer system.

$F_S =$ noise factor of end-to-end simple, single-channel system.

$F_{WDM} =$ noise factor of end-to-end single-channel WDM system.

$F_{BF} =$ noise factor of end-to-end BF system.

$G_{lna} =$ RF gain of LNA.

$G_{lna,m} =$ RF gain of $m-th$ LNA.

$G_{pho} =$ RF gain of photonic section only, referenced to MZM i/p.

$G_{pho,m} =$ RF gain of photonic section only of the $m-th$ channel wrt MZM i/p.

$G_{pho-S} =$ RF gain for a simple, single channel link wrt MZM i/p.

$G_{pho-wdm} =$ RF gain for a single-channel WDM link wrt MZM i/p.

$G_{BF} =$ End-to-end RF gain of BF system.

$G_S =$ End-to-end RF gain of simple, single-channel link $= G_{lna}G_{pho-S}$.

$G_{WDM} =$ End-to-end RF gain of single-channel WDM link $= G_{lna}G_{pho-wdm}$.

$i_{out} =$ total photocurrent.

$i_{out,m} =$ photocurrent due to $m-th$ channel.

$i_{RF} =$ RF photocurrent

$i_{RF0} =$ amplitude of RF photocurrent.

$i_{RF,m} =$ RF photocurrent due to $m-th$ channel $= i_{RF0,m}\sin(\Omega t - \theta_m)$.

$i_{RF0,m} =$ amplitude of RF photocurrent at PD output due to $m-th$ laser.

$I_{DC} =$ DC photocurrent

$I_{DC,m} = \frac{1}{K}\left(\frac{\Re p_m}{\alpha_m}\right) =$ In BF system, DC photocurrent due to $m-th$ laser .

$I_{DC-S} = \left(\frac{\Re p}{\alpha}\right) =$ DC photocurrent due to ONE laser with rms opt. power p.

$I_{DC-S,m} = \left(\frac{\Re p_m}{\alpha_m}\right) =$ DC photocurrent due to $m-th$ laser.

$K =$ # beamformer modules.

$k_B =$ Boltzmann constant.

$LNA =$ low-noise amplifier

$M =$ # of array antenna elements in BF system = # lasers in BF system.

$N_{out} =$ noise power spectral density (W / Hz) at PD o/p.

$N_{bf,m} =$ noise PSD at BFM output due to $m-th$ channel.

$N_{BF} =$ total noise PSD at BFM o/p.

$N_S =$ total noise PSD at simple, single-channel link o/p.

$N_{WDM} =$ total noise PSD at single-channel WDM link o/p.

$N_{pho-S} =$ o/p noise PSD for photonic portion of simple, single-channel link.

$N_{pho-wdm} =$ o/p noise PSD for photonic portion of single-channel WDM link.

$NF =$ noise figure.

$P_{in} =$ input RF rms electrical power .

$P_{out} =$ output RF rms electrical power.

$p =$ optical power from laser source at MZM input.

$p_m =$ optical power from $m-th$ laser source at MZM_m input.

$PD =$ photodetector.

$PSD =$ power spectral density $(W / Hz = J)$

$q =$ electron charge = $1.6e-19\ C$.

$RIN =$ relative-intensity-noise PSD normalized to DC electrical power.

$RIN_m =$ RIN of $m-th$ laser.

$T_0 =$ standard temperature = $290K$.

$v =$ RF voltage at MZM input $= v_0 \sin(\Omega t - \psi)$.

$v_m =$ RF voltage at MZM_m input $= v_{0m} \sin(\Omega t - \psi_m)$

$v_{in} =$ input voltage

$v_{lna} =$ RF voltage at LNA input $= v_{lna0} \sin(\Omega t - \psi)$.

$v_{lna0} =$ amplitude of RF voltage at LNA input.

$v_{lna,m} =$ RF voltage at input to $m-th$ LNA $= v_{lna0,m} \sin(\Omega t - \psi_m)$.

$v_{lna0,m} =$ amplitude of RF voltage at $m-th$ LNA input.

$v_0 =$ amplitude of RF voltage at MZM input = $\sqrt{G_{lna}} v_{lna0}$.

$v_{0m} =$ amplitude of RF voltage at $m-th$ MZM input = $\sqrt{G_{lna,m}} v_{lna0,m}$.

$V_\pi =$ MZM half-wave voltage.

$V_{\pi,m} =$ half-wave voltage of $m-th$ MZM.

$v_{vna} =$ RF voltage at VNA output $= v_{vna0} \sin \Omega t$.

$v_{vna0} =$ amplitude of RF voltage at VNA output.

Distribution Statement A. Approved for public release, distribution is unlimited.

$VNA =$ vector network analyzer.

$Z_{in} =$ input load impedance.

$Z_{out} =$ PD output load impedance.

$\alpha =$ optical power attenuation factor ($\alpha \geq 1$).

$\alpha_m =$ optical power attenuation factor in $m-th$ channel ($\alpha_m \geq 1$).

$\Delta\theta_{nm} = \theta_n - \theta_m$.

$\kappa = |E|^2/2p =$ constant relating optical power p to $|E|^2$.

$$\rho = \begin{cases} 1 & \text{at DC,} \\ 1 & \text{at RF if PD has no internal load,} \\ 1/2 & \text{at RF if PD has internal load.} \end{cases}$$

$\psi_m =$ phase of RF signal at $m-th$ receive antenna.

$\theta_m =$ RF phase of signal from $m-th$ channel at BFM output.

$\phi =$ optical phase impressed on optical carrier by voltage input to MZM.

$\phi_{bias} =$ DC optical phase.

$\phi_{RF} =$ RF optical phase.

$\lambda =$ laser wavelength.

$\lambda_m =$ wavelength of $m-th$ laser.

$\Omega =$ RF (radian) frequency.

$\mathcal{R} =$ responsivity of PD.

$\mathcal{B}(M) = 2 \times$ magnitude squared of coherent sum of RF photocurrents.

B APPENDIX B: ANALYSIS OF E-FIELDS IN SIMPLE, SINGLE-CHANNEL LINK

In the diagram on the next page we present some details of the standard analysis of a simple, single RF-channel link at the level of E-fields.

Distribution Statement A. Approved for public release, distribution is unlimited.

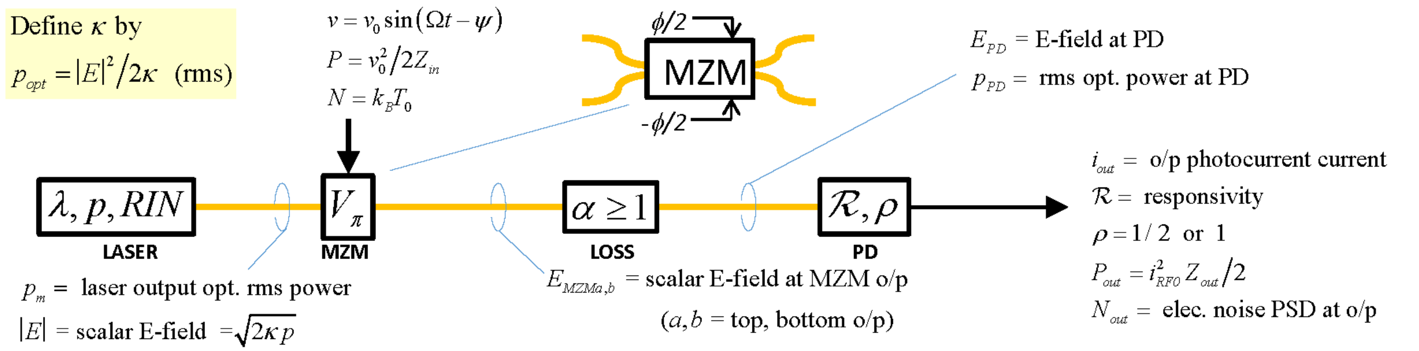

For balanced, push-pull MZM: $\begin{bmatrix} E_{MZMa} \\ E_{MZMb} \end{bmatrix} = j \begin{bmatrix} \sin(\phi/2) & \cos(\phi/2) \\ \cos(\phi/2) & -\sin(\phi/2) \end{bmatrix} \begin{bmatrix} E_1 \\ E_2 \end{bmatrix}$ where $\phi \begin{cases} = \phi_{bias} + \phi_{RF} \\ = \dfrac{\pi}{V_\pi(0)} V_{DC} + \dfrac{\pi}{V_\pi(\Omega)} v_0 \sin(\Omega t - \theta) \end{cases}$

Hence $\begin{bmatrix} E_{MZMa} \\ E_{MZMb} \end{bmatrix} = j \begin{bmatrix} E_1 \sin(\phi/2) + E_2 \cos(\phi/2) \\ E_1 \cos(\phi/2) - E_2 \sin(\phi/2) \end{bmatrix} \xrightarrow{E_2 = 0} jE_1 \begin{bmatrix} \sin(\phi/2) \\ \cos(\phi/2) \end{bmatrix} \xrightarrow{E_1 = \sqrt{2\kappa p}} j\sqrt{2\kappa p} \begin{bmatrix} \sin(\phi/2) \\ \cos(\phi/2) \end{bmatrix}$

Note : ρ multiplies only the RF term.

Choose one of the MZM o/ps, say, $E_{MZMb} = j\sqrt{2\kappa p} \cos\left(\dfrac{\phi}{2}\right)$. Then $E_{PD} = j\sqrt{\dfrac{2\kappa p}{\alpha}} \cos\left(\dfrac{\phi}{2}\right) \Rightarrow p_{PD} = \dfrac{1}{2\kappa}|E_{PD}|^2 = \dfrac{p}{\alpha}\cos^2\left(\dfrac{\phi}{2}\right) = \dfrac{p}{\alpha}(1 + \cos\phi)$.

Under the usual assumptions (quadrature, small-signal): $p_{PD} = \dfrac{p}{\alpha}\left[1 + \phi_{RF,0} \sin(\Omega t - \theta)\right]$.

$$i_{out} = \mathcal{R} p_{PD} = \frac{\mathcal{R} p}{\alpha}\left[1 + \rho \phi_{RF0} \sin(\Omega t - \theta)\right] = I_{DC-S} + i_{RF0} \sin(\Omega t - \theta)$$

$$P_{out,m} = \frac{i_{RF0}^2 Z_{out}}{2} = \frac{Z_{out}}{2}\left(\frac{\mathcal{R}\rho p}{\alpha}\right)^2 \phi_{RF0}^2 = \frac{Z_{out}}{2} I_{DC-S}^2 \left(\frac{\pi\rho}{V_\pi(\Omega)} v_0\right)^2$$

$$with\ P_{in} = \frac{v_0^2}{2Z_{in}} \Rightarrow \begin{cases} G = \dfrac{Z_{out}}{2} I_{DC-S}^2 \left(\dfrac{\pi\rho}{V_\pi(\Omega)} v_0\right)^2 \dfrac{2Z_{in}}{v_0^2} \\ = \left(\dfrac{\pi^2 Z_{in} Z_{out} \rho^2}{V_\pi^2(\Omega)}\right) I_{DC-S}^2 \\ \equiv \gamma I_{DC}^2 \end{cases}$$

C APPENDIX C: ALTERNATE DERIVATION OF THE BEAMFORMER EQUATION

In this Appendix we provide an alternate derivation of the beamformer result Eq.(47). The RF portion of the photocurrent i_{out} in Eq.(41) is

$$\sum_{m=1}^{M} i_{RF,m} = \sum_{m=1}^{M} i_{RF0,m} \sin\left(\Omega t - \theta_m\right). \tag{65}$$

Since each sinusoidal term in the summation has the same RF frequency, the sum itself can be written as a single sinusoid by first expanding $\sin\left(\Omega t - \theta_m\right) = \sin\Omega t \cos\theta_m - \cos\Omega t \sin\theta_m$ and then

$$\sum_{m=1}^{M} i_{RF0,m} \sin\left(\Omega t - \theta_m\right) = i_{RFtot} \sin\left(\Omega t - \Theta\right). \tag{66}$$

where

$$i_{RFtot}^2 = \left(\sum_{m=1}^{M} i_{RF0,m} \cos\theta_m\right)^2 + \left(\sum_{m=1}^{M} i_{RF0,m} \sin\theta_m\right)^2 \tag{67}$$

and

$$\tan\Theta = \frac{\sum_{m=1}^{M} i_{RF0,m} \sin\theta_m}{\sum_{m=1}^{M} i_{RF0,m} \cos\theta_m}. \tag{68}$$

Written in this way, the RF output power is

$$P_{out} = \frac{1}{2} i_{RFtot}^2 Z_{out}. \tag{69}$$

Assume that the amplitudes of the photocurrent contributions from each path are equivalent, $i_{RF0,m} = i_{RF0}$ for all m. Then the sums

$$i_{RFtot}^2 = i_{RF0}^2 \left[\left(\sum_{m=1}^{M} \cos\theta_m\right)^2 + \left(\sum_{m=1}^{M} \sin\theta_m\right)^2\right] \tag{70}$$

can be evaluated as follows:

$$i_{RFtot}^2 = i_{RF0}^2 \left[\sum_{m=1}^{M} \left(\cos^2\theta_m + \sin^2\theta_m\right) + \sum_{m\neq n=1}^{M} \cos\theta_m \cos\theta_n + \sum_{k\neq l=1}^{M} \sin\theta_k \sin\theta_l \right]. \tag{71}$$

But $\cos^2\theta_m + \sin^2\theta_m = 1$ for all m and, by properly pairing up terms,

$$\sum_{m\neq n=1}^{M} \cos\theta_m \cos\theta_n + \sum_{k\neq l=1}^{M} \sin\theta_k \sin\theta_l = \sum_{m\neq n=1}^{M} \cos\left(\theta_n - \theta_m\right). \tag{72}$$

Hence,

$$i_{RFtot}^2 = i_{RF0}^2 \left[M + \sum_{m\neq n=1}^{M} \cos\left(\theta_n - \theta_m\right) \right]. \tag{73}$$

where the sum here contains $\left(M^2 - M\right)$ terms. This is the same result as in (47).

Distribution Statement A. Approved for public release, distribution is unlimited.

References

[1] M.J. Mondich, J.D. McKinney, F. Bucholtz, J.M. Singley, I.M. Maize, and K.J. Williams. "Group delay based wideband photonic receive mode radio frequency beamforming". *Accepted for publication in J. Lightwave Technol. doi: 10.1109/JLT.2020.3005900.* X (2020), p. X.

[2] J.M. Singley, V.J. Urick, J.F. Diehl, K.J. Williams, and F. Bucholtz. "Increased performance of single-channel analog photonic links enabled by optical wavelength-division multiplexing". *IEEE Trans. Micro. Theory Tech.* 67 (3) (2019), pp. 1274–1282.

[3] N.M. Froberg, E.I. Ackerman, and C.H. Cox, III. "Analysis of signal to noise ratio in photonic beamformers". *Aerospace Conference 2006* (2006), 12 pgs.

[4] F. Bucholtz, M.J. Mondich, J.M. Singley, J.D. McKinney and K.J. Williams. "The noise figure for multiple-input RF systems". *NRL/MR/5651–20-10,103* (28 Aug 2020), 45 pgs.

[5] V.J. Urick, Jr., J.D. McKinney, and K.J.Williams. *Fundamentals of microwave photonics*. Wiley, 2015.

[6] C.H. Cox, III. *Analog optical links*. Cambridge, 2004.

[7] W.S.C. Chang. *RF photonic technology in optical fiber links*. Cambridge, 2002.

[8] F. Bucholtz, V.J. Urick, M. Godinez and K.J. Williams. "Graphical approach for evaluating performance limitations in externally-modulated analog photonic links". *IEEE Trans. Microw. Theory Techn.* 56 (1) (2008), pp. 242–247.

Distribution Statement A. Approved for public release, distribution is unlimited.